

See discussions, stats, and author profiles for this publication at: <https://www.researchgate.net/publication/51116140>

# Differences in Metabolism between the Biofilm and Planktonic Response to Metal Stress

ARTICLE *in* JOURNAL OF PROTEOME RESEARCH · MAY 2011

Impact Factor: 4.25 · DOI: 10.1021/pr2002353 · Source: PubMed

CITATIONS

50

READS

81

8 AUTHORS, INCLUDING:



[Sean Cameron Booth](#)

The University of Calgary

9 PUBLICATIONS 83 CITATIONS

[SEE PROFILE](#)



[Rustem Shaykhutdinov](#)

The University of Calgary

31 PUBLICATIONS 1,168 CITATIONS

[SEE PROFILE](#)



[Raymond J. Turner](#)

The University of Calgary

172 PUBLICATIONS 4,525 CITATIONS

[SEE PROFILE](#)



[Aalim Weljie](#)

University of Pennsylvania

71 PUBLICATIONS 3,078 CITATIONS

[SEE PROFILE](#)

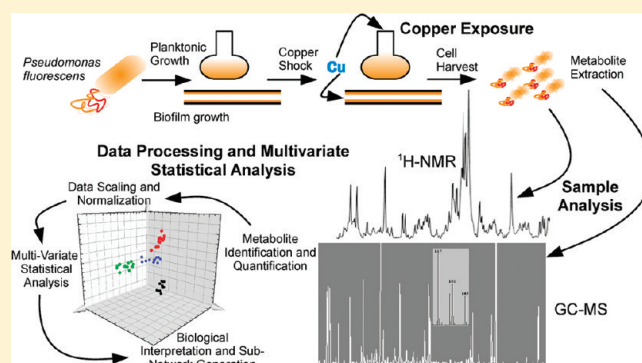
## Differences in Metabolism between the Biofilm and Planktonic Response to Metal Stress

Sean C. Booth,<sup>†</sup> Matthew L. Workentine,<sup>†,‡</sup> Jing Wen,<sup>§</sup> Rustem Shaykhutdinov,<sup>§</sup> Hans J. Vogel,<sup>†,§</sup> Howard Ceri,<sup>‡</sup> Raymond J. Turner,<sup>†,‡</sup> and Aalim M. Weljie<sup>\*,†,§</sup>

<sup>†</sup>Department of Biological Sciences, <sup>‡</sup>Biofilm Research Group, and the <sup>§</sup>Metabolomics Centre, University of Calgary, Calgary, AB, Canada T2N 1N4

**ABSTRACT:** Bacterial biofilms are known to withstand the effects of toxic metals better than planktonic cultures of the same species. This phenomenon has been attributed to many features of the sessile lifestyle not present in free-swimming populations, but the contribution of intracellular metabolism has not been previously examined. Here, we use a combined GC–MS and <sup>1</sup>H NMR metabolomic approach to quantify whole-cell metabolism in biofilm and planktonic cultures of the multimetal resistant bacterium *Pseudomonas fluorescens* exposed to copper ions. Metabolic changes in response to metal exposure were found to be significantly different in biofilms compared to planktonic cultures. Planktonic metabolism indicated an oxidative stress response that was characterized by changes to the TCA cycle, glycolysis, pyruvate and nicotinate and niacinamide metabolism. Similar metabolic changes were not observed in biofilms, which were instead dominated by shifts in exopolysaccharide related metabolism suggesting that metal stress in biofilms induces a protective response rather than the reactive changes observed for the planktonic cells. From these results, we conclude that differential metabolic shifts play a role in biofilm-specific multimetal resistance and tolerance. An altered metabolic response to metal toxicity represents a novel addition to a growing list of biofilm-specific mechanisms to resist environmental stress.

**KEYWORDS:** biofilm, *Pseudomonas fluorescens*, copper resistance, metabolomics, metabolism, metal resistance, biofilm physiology, environmental toxicology, toxicometabolomics



### INTRODUCTION

Even after years of study, bacterial biofilms remain a frontier of microbiology as they exhibit many industrial, environmental and medically important properties not displayed by their planktonic counterparts which have yet to be fully explained.<sup>1</sup> One such property is the increased tolerance and resistance of biofilms to concentrations of toxic metals compared to planktonic cultures.<sup>2</sup> This has been attributed to several factors inherent to the biofilm lifestyle including quorum-sensing mediated gene regulation, metal chelation by the extracellular polymeric substance (EPS), and increased persister cell formation.<sup>2</sup> Another important factor is the presence of phenotypic and metabolic heterogeneity within the biofilm environment.<sup>3</sup> This heterogeneity is considered to be caused by gradients of pH, oxygen, and nutrients in the biofilm matrix not present in planktonic cultures.<sup>3</sup> Given that these factors all have an impact on cellular metabolism, it can be expected that metabolism occurring in biofilms would be different than in planktonic cultures, and hence, it may also be a factor in their differential tolerance/resistance to metal ions.

Metabolism represents one of the most dynamic aspects of cellular physiology and by studying it directly one can obtain a unique snapshot of underlying physiological processes.<sup>4</sup> Metabolomics has grown in recent years as a powerful tool both for complementing other 'omic' studies and for investigating the

immense metabolic diversity found in prokaryotes.<sup>5</sup> It has been used to study the effects of antibiotics in *Mycobacterium tuberculosis*,<sup>6</sup> to compare ethanol and iron-limitation stress in *Staphylococcus aureus*,<sup>7</sup> and to identify metabolic differences between biofilms and planktonic cultures of *Pseudomonas aeruginosa*.<sup>8</sup> Additionally, previous studies by our group have revealed significant metabolic differences between different *Pseudomonas fluorescens* mutant strains and between *Pseudomonas pseudoalcaligenes* KF707 strains exposed to tellurite using a proton nuclear magnetic resonance (<sup>1</sup>H NMR) based technique on planktonic cultures.<sup>9</sup>

Although <sup>1</sup>H NMR is commonly used for metabolomic analyses,<sup>10</sup> it is still hampered by insensitivity and difficulty in identification of low concentration metabolites. Gas chromatography–mass spectrometry (GC–MS), also frequently used for metabolomics, is highly sensitive with semi-automated metabolite identification capabilities, though it is somewhat less quantitative. Here, we present their combined use as an improved adaptation over prior microbial metabolomics studies.<sup>9</sup> *P. fluorescens* is an excellent model organism for this study due to its varied metabolic capabilities<sup>11</sup> and its well-studied interactions with toxic metals. A brief sampling of these studies includes a systematic exposure to

Received: March 14, 2011

Published: May 12, 2011

much of the periodic table,<sup>12</sup> its ability to detoxify selenite and mercury,<sup>13</sup> and its resistance to aluminum.<sup>14</sup> To garner an understanding of the differences between biofilm and planktonic culture's metabolic response to copper, tube-reactor grown biofilms and shaker-flask grown planktonic cultures were exposed to a sublethal copper shock then harvested for their intracellular metabolites to be analyzed. Our results indicate that the response in each culture type is quite distinct and the differences provide insights into factors that provide biofilm metal resistance.

## ■ EXPERIMENTAL PROCEDURES

### Planktonic Culture Growth

*P. fluorescens* ATCC 13525 from  $-80^{\circ}\text{C}$  freezer stock was subcultured twice, first on LB agar then in 5 mL of LB broth overnight. Planktonic cultures were prepared by inoculating 50 mL of LB with 500  $\mu\text{L}$  of the overnight subculture and growing for 24 h at  $30^{\circ}\text{C}$  with shaking (200 rpm). After 24 h of growth, half of the cultures were copper-shocked by adding  $\text{CuSO}_4$  to a final concentration of 1.5 mM, which is approximately half the minimum inhibitory concentration.<sup>12</sup> Sterile water was added to the other half of the cultures, which were the controls. Cultures were exposed to copper for 4 h followed by harvest. Immediately prior to harvest, the cell density was measured at OD 600 to ensure that the exposure was not causing a significant decrease. On the basis of prior work, the concentration used is not toxic enough to cause significant cell death.<sup>12</sup> Cell harvest was performed as previously described,<sup>9a</sup> using  $-50^{\circ}\text{C}$  60% methanol to quench the cells. Following quenching and centrifugation, the cell pellet was stored at  $-80^{\circ}\text{C}$  until further use. Four technical replicates of three biological replicates were prepared for each condition for a total of 12 samples of each condition.

### Biofilm Culture Growth

Biofilms were grown on the inside of silicone tubing in a method similar to that previously described.<sup>15</sup> LB media from a reservoir was pumped through 4 identical 1 m long silicone tubing (i.d. 0.187 mm) preceded by a bubble trap. After initial setup, the tubing was inoculated with 10 mL of overnight subculture using a 30 gauge needle. This was allowed to sit for 2 h to allow the cells to attach to the tubing wall, then the flow was started at approximately 0.5 mL/min. Biofilms were grown for 48 h at which point the media reservoir for two of the tubes was switched to LB containing 1.5 mM  $\text{CuSO}_4$ . Flow was started again and the biofilms were grown for another 24 h. Both the growth time and exposure time were adjusted for the biofilms to allow for the slower growth as compared to the planktonic cells. We found that this growth time was necessary in order to allow sufficient biomass to accumulate on the interior of the tubing. Previous work by our group has indicated that 24 h exposure time for biofilms is sufficient to allow the metal ion to induce a toxic response.<sup>16</sup> To harvest, excess media and loosely attached cells were allowed to drain from the tubing, then the tubes were divided into three equal parts. The cell mass was extruded from each tube section using a metal clamp into preweighed microfuge tubes. The cells were then rapidly frozen in liquid nitrogen and stored at  $-80^{\circ}\text{C}$  until further use. In this manner, each biofilm experiment provided, for each condition, two biological replicates each consisting of three technical replicates for a total of 12 samples.

### Metabolite Extraction

Previous metabolomic work performed by our group used a protocol for metabolite extraction with methanol that was

developed in our lab.<sup>9a</sup> With increased experience, this protocol has been optimized and modified as described here to improve sample handling and efficiency. The extraction procedure described is a modification of a previous protocol.<sup>17</sup> Cell pellets from both biofilms and planktonic cells were thawed on ice and then resuspended in 300  $\mu\text{L}$  of a 2:1 methanol/chloroform mixture by pipetting. Samples were transferred to fresh microfuge tubes and cells were lysed by sonication for 15–20 s at a 10 W power setting. To this, 100  $\mu\text{L}$  of each layer from a chloroform/water solution was added and mixed gently by inversion. The aqueous and organic layers were separated by centrifugation in a microfuge at 14 000 rpm for 7 min at  $4^{\circ}\text{C}$ . The top aqueous layer was removed to a clean tube and centrifuged again to remove any remaining organic phase. One-third (100  $\mu\text{L}$ ) of the aqueous phase was placed in a separate tube for GC–MS analysis with remaining two-thirds to be used for NMR analysis. All samples were dried down in a vacuum concentrator for 4 h, then stored at  $-80^{\circ}\text{C}$  until analysis.

### NMR Acquisition and Data Processing

Samples were prepared for NMR analysis and acquisition parameters for one-dimensional  $^1\text{H}$  NMR were as previously described.<sup>9a</sup> Immediately prior to analysis, samples were thawed and the pH was adjusted to  $7.00 \pm 0.05$  with small amounts of NaOH or HCl. A chemical shift standard (2,2-dimethyl-2-silapentane-5-sulfonate, DSS) was added to a final concentration of 0.25 mM in a total of 1 mL of  $\text{D}_2\text{O}$ . A 600  $\mu\text{L}$  aliquot of sample was loaded into an NMR tube for analysis.  $^1\text{H}$  NMR spectra were acquired on a 600-MHz BrukerAvance II spectrometer using a standard nuclear Overhauser effect spectroscopy (NOESY) presaturation experiment from the Bruker pulse program library (noesypr1d), with an initial relaxation delay of 3 s and an acquisition time of 2 s for an overall recycle time of 5 s. A delay of 100 ms was used for the NOESY mixing time. Additional two-dimensional NMR experiments were performed for the purpose of confirming chemical shift assignments, including total correlation spectroscopy (2D  $^1\text{H}$ – $^{13}\text{C}$  TOCSY) and heteronuclear single quantum coherence spectroscopy (2D  $^1\text{H}$ – $^{13}\text{C}$  HSQC), using standard Bruker pulse programs. Processed spectra were imported into Chenomx NMR Suite 5.1 (Chenomx, Edmonton, Alberta). Phase and baseline were manually corrected, then individual peak assignments were made by comparison to a standard library. Compounds with only 1 peak were verified by analysis of the 2D spectra. Concentrations of individual metabolites were determined using the ‘targeted profiling’ method which compares the integrals of identified compounds to a known reference signal.<sup>18</sup> Compound concentrations were exported for further statistical analysis.

### GC–MS Acquisition and Data Processing

Dried metabolite extracts were derivatized according to the literature.<sup>19</sup> Briefly, 50  $\mu\text{L}$  of 20 mg/mL methoxyamine (Sigma Aldrich) in pyridine was added to the dried sample and incubated for 2 h at  $37^{\circ}\text{C}$ . This was followed by the addition of 50  $\mu\text{L}$  of *N*-methyl-*N*-trimethylsilyltrifluoroacetamide (MSTFA, Sigma Aldrich) and incubation at  $37^{\circ}\text{C}$  for another 45 min. Samples were diluted with hexane and 150  $\mu\text{L}$  was transferred to the GC–MS autosampler vial. Analysis was carried out on a Waters GCT premier mass spectrometer using helium as the carrier gas at a constant flow of  $1.2\text{ mL min}^{-1}$ . The MS was operated in a range of 50–800  $m/z$ . A total of 1  $\mu\text{L}$  of derivatized sample was injected into a  $30\text{ m} \times 0.25\text{ mm i.d.} \times 0.25\text{ }\mu\text{m}$  DB5-MS column using splitless injection. The injector temperature was  $275^{\circ}\text{C}$

and the initial column temperature of 80 °C was held for 1 min then ramped at 12 °C min<sup>-1</sup> to 320 °C and held for 8 min.

Spectral deconvolution and calibration was performed using AMDIS and a set of alkane standards to obtain retention index (RI) values along with the corresponding mass spectrum. The output from AMDIS was then input to MET-IDEA in order to identify the components that are conserved in all the spectra. MET-IDEA uses a high quality representative spectra to build a list containing ion/retention time pairs (IRT).<sup>20</sup> The software selects the appropriate model ion for each retention time according to a variety of parameters. A retention time correction is performed for all the samples, then the IRT list is used as reference against which the remaining spectra are queried and a file containing the abundance information for each metabolite in all the samples is assembled. This file is then used for further statistical analysis.

### Statistical Analysis

Data transformations and manipulations were done using Excel 2008 (Microsoft, Redmond, WA), multivariate statistical analysis was performed with SIMCA-P (Umetrics) and Significance Analysis of Microarrays (SAM), and hierarchical clustering was performed with MeV 4.4.1.<sup>21</sup> Prior to analysis, both sets of data (GC–MS and NMR) were normalized by dividing the abundance of each metabolite by the sum of all the metabolites in that spectrum. This was done to account for any differences in global sample concentrations resulting from differential cell masses in the samples. Both sample sets were individually scaled with the SIMCA-P software using unit variance scaling followed by mean centering, which is known to be an effective scaling method.<sup>22</sup> This allows for the direct comparison of the GC–MS and NMR data sets. Prior to compound identification, the scaled and normalized GC–MS data were filtered to remove nonsignificant and noisy components by identifying significant metabolites using multiclass SAM with a false discovery rate (FDR) of <1% and by partial least-squares discriminant analysis (PLS-DA) to identify metabolites with a variable influence on projection (VIP) of >1. The significant metabolites from each method were combined, and in this way, the initial list of ~500 components from the GC–MS spectra was reduced to ~200. Metabolites from the GC–MS spectra were identified by searching the NIST library and the GOLM Metabolite Database.<sup>23</sup> Components that were identified as the same compound were averaged. This list of identified compounds was combined with the NMR data set and any compounds that were the same (had the same KEGG ID) were averaged. This list was then analyzed with various statistical techniques. Hierarchical cluster analysis was performed using Pearson correlation as the distance measure.

## RESULTS

For the planktonic cells, cultures were grown for 24 h followed by a 4 h exposure to a sublethal concentration of copper. Biofilms were established on the inside of silicone tubes for 48 h followed by a 24 h exposure to sublethal copper concentration. The differences in growth and exposure times were necessary due to the slow-growing nature of biofilms. The cells were harvested and rapidly frozen followed by separation from the media and subsequent lysis. The intracellular metabolites were then extracted and divided for separate analysis. Metabolites in the samples were quantified using both <sup>1</sup>H NMR and GC–MS analysis. These data sets were then combined, and the mean of scaled value was used when both techniques identified the same

metabolite. This produced a list of 79 metabolites, which was used for all further analysis.

To get an overall picture of the important metabolic changes, the metabolites were analyzed by SAM (Significance Analysis of Microarrays) and subsequently clustered (Figure 1). The most clear metabolic differences occurred between biofilm and planktonic cultures, which is expected but has yet to be characterized in this fashion and was surprising how different the metabolism is. However, there were also large differences between the control and copper exposed biofilm samples whereas the metabolic differences between the control and copper exposed planktonic samples were less pronounced, although still observable. Unexpectedly, under copper stress the metabolite profiles did not converge, instead they were quite distinct. The clustering identified 3 main groups of metabolites (these groups are defined in the colored groupings in Figure 1): metabolites that only changed in the planktonic samples, metabolites that only changed in the biofilm samples and those that changed in both. The metabolites changing in the biofilm samples can also be subdivided into those that increased and those that decreased in response to copper exposure. While the clustering did show significant differences between sample classes, more robust statistical methods were undertaken to examine the metabolic changes induced by copper.

Principal component analysis (PCA) was used to identify significant differences in the data set (Figure 2a). PCA is an unsupervised, reductive statistical modeling technique that separates samples based on their differences from each other. The biofilm samples clearly separated between control and copper exposed samples, whereas the planktonic samples did not separate at all. Partial least-squares discriminant analysis (PLS-DA) is similar but is supervised, allowing for the definition of classes before the test is performed. This allowed the differences between the two planktonic classes to become apparent (Figure 2b). While the planktonic control and copper exposed samples are separated in the 3D scatter plot, they are clearly less tightly clustered than both classes of biofilm samples. The calculated *R*<sup>2</sup> and *Q*<sup>2</sup> values, which respectively indicate goodness of fit and cross validation predictive ability for the PCA and PLS-DA are seen in Table 1. Ideal values are close to 1, but this is rare and unlikely in biological systems. For the PCA and PLS-DA models, these values indicate that there are statistically significant differences between the samples.

As would be expected, the largest difference in the data was between the biofilm and planktonic samples. As such, individual pairwise OPLS-DA models were generated to examine the specific differences between the individual growth modes, that is, the planktonic response to copper was analyzed independently of the biofilm samples and vice versa. OPLS-DA maximizes the variation between the specified groups and minimizes the variation between the individual replicates. It therefore highlights the important differences between the two compared sample classes. The statistics for these models are also given in Table 1. For each of the OPLS-DA models, two values were calculated which help determine which metabolites are important for the response to copper. The variable influence on projection (VIP) gives an indication of each metabolite's significance to that model. A metabolite with a VIP of greater than 1 is considered to have a statistically significant contribution to the model.<sup>24</sup> The other informative value from the OPLS-DA model is the metabolite coefficient, which gives an indication of the direction and magnitude of change. For both models, a positive coefficient



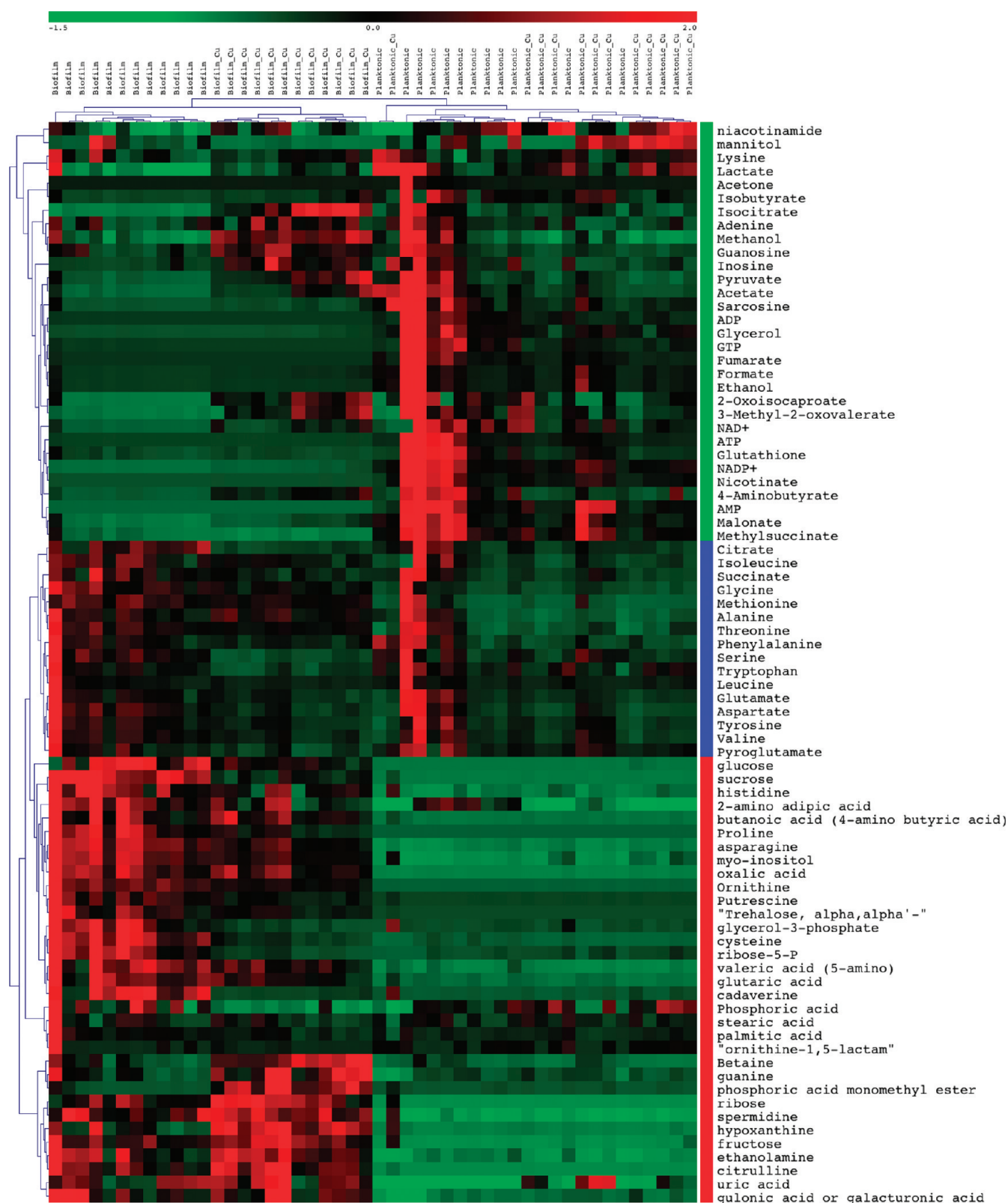


**Figure 1.** Hierarchical clustering analysis of control and copper exposed biofilm and planktonic culture metabolite concentrations. Identified metabolites were analyzed for any apparent patterns. Clustering was performed using Pearson correlation as the distance metric. The cluster tree shows how the samples and metabolites divide. Across the top are the samples, labeled by their class and along the side are the metabolites. These were colored according to the grouping pattern that they showed: green metabolites were only changing in the planktonic cultures, red only in biofilms and blue were changing in both cultures in response to copper exposure.

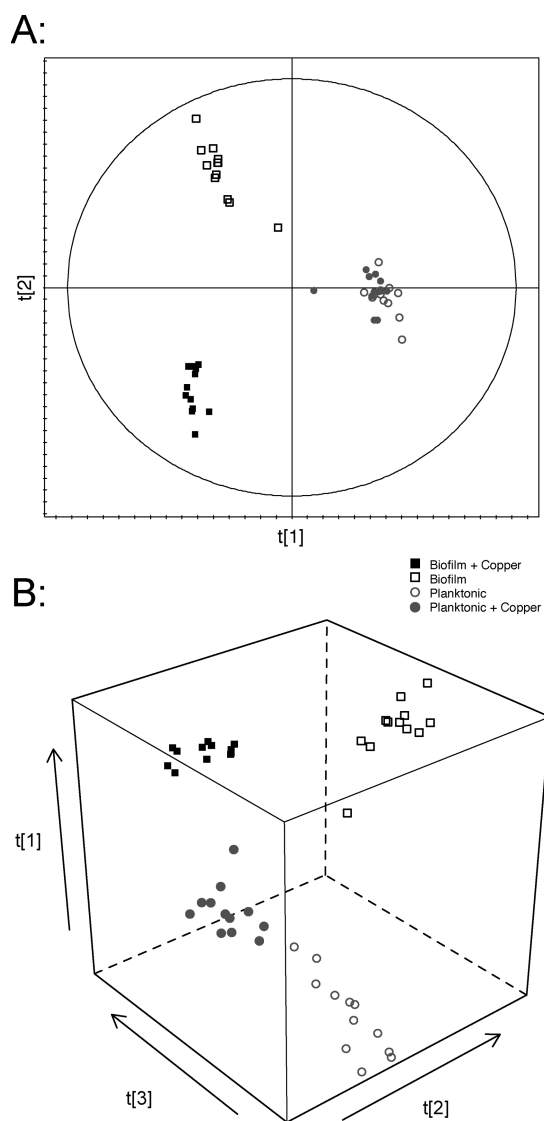


**Figure 2.** Principal component analysis (PCA) and partial least-squares discriminant analysis (PLS-DA) scatter plots of *P. fluorescens* cultures. (A) Control biofilm (open square) and copper exposed biofilm (filled square) show clear separation whereas the control planktonic (open circle) and copper exposed planktonic (filled circle) are not separated at all. While the calculated model had 3 components (Table 1), the third component did not separate any of the samples much further than the first 2 already had. (B) In the 3D PLS-DA plot, samples were labeled according to class before analysis, resulting in separation of all samples along a combination of the three component axes. While the biofilm samples (squares) respectively clustered tightly, the planktonic samples (circles) were more loosely grouped.

indicates that the metabolite is increasing upon exposure to copper and a negative coefficient means that metabolite is decreasing. Using these values, shared-and-unique structure (SUS) plots<sup>25</sup> were constructed comparing the biofilm and planktonic VIP values and coefficients (Figure 3). In these plots, the VIP and coefficients from the two separate OPLS-DA models are plotted against each other to determine what, if any, changes are common to both the planktonic and biofilm response to copper. The VIP comparison (Figure 3a) shows only 3 metabolites have above average significance between the two responses: NAD<sup>+</sup>, phosphoric acid, and glutathione, highlighting the fact

that the biofilms and planktonic response to copper are quite distinct from each other. The comparison of OPLS-DA coefficients (Figure 3b) displays an interesting difference between the two data sets. Metabolites were colored according to in which growth mode their VIP score was above 1. Metabolites deemed significant in the biofilm model (squares) had relatively smaller coefficients in the planktonic model, and vice versa for the significant metabolites in the planktonic model (circles).

The metabolite's classification determined from the clustering was also used to see if and how these compounds were related in real metabolic networks. To this end, each list of metabolites was submitted to TICL (the Tool for automatic Interpretation of a Compound Library).<sup>26</sup> This Web-tool uses the KEGG library of metabolic maps to link a list of compounds into a subnetwork even if there are intermediate compounds missing and also determines which metabolic pathways are most likely to be involved with these compounds. The three metabolite lists (corresponding each to important in the biofilm, planktonic and combined response to copper exposure) were individually submitted to TICL and the results of this analysis are shown in Table 2. These results again show that the response to copper stress is very different between biofilms and planktonic cultures, but also shows that there is a shared response. Specifically, the planktonic response involves changes to nicotinate, pyruvate, and purine metabolism and changes to the TCA cycle and glycolysis. The biofilm response is more involved with galactose and sucrose metabolism and the phosphotransferase system. The combined response, which had the smallest pool of input compounds, produced the most affected metabolic networks involving various aspects of amino acid biosynthesis and metabolism. One interesting aspect of this analysis was that there were no networks identified in all three responses, but glutathione metabolism was conserved between biofilms and the combined response and alanine, aspartate, and glutamate metabolism and valine, leucine, and isoleucine biosynthesis were conserved between planktonics and the combined response.

## DISCUSSION

Metabolomics is a rapidly developing field with a plethora of applications; however, there have been few studies published on the metabolomics of bacteria growing as a biofilm. Here, we present the first use of metabolomics to investigate the effects of a toxic stressor on bacterial biofilms by using a combined <sup>1</sup>H NMR and GC-MS approach to identify differences in the response to copper stress between biofilms and planktonic cultures. We found that there are major metabolic differences between biofilms and planktonic cultures and also that the metabolic changes induced by exposure are dramatically different between the two growth modes.

Metal ions are being revisited for antimicrobial applications, and copper shock has been found to alter the expression of a large number of genes in *P. aeruginosa*.<sup>27</sup> Such a large change in gene expression would also be indicative of a significant metabolic shift. The physical chemistry associated with metal toxicity has been found to be different in biofilms compared to planktonic cultures.<sup>12</sup> On the basis of these previous studies, we hypothesized that copper exposure would significantly alter the *P. fluorescens* metabolome but it was unknown exactly how each growth mode would respond. A convergence of metabolomes could have been expected as each culture type was dealing with same toxic stressor. Instead, a specific, distinct response was

Table 1. Statistical Values Associated with Multivariate Statistical Models

Model Description	Type	Model Type	Components	Model Statistics	
				R <sup>2</sup>	Q <sup>2</sup>
Planktonic and Biofilm $\pm$ Cu	Unsupervised	PCA-X	3	0.692	0.580
Planktonic and Biofilm $\pm$ Cu	Supervised	PLS-DA	3	0.681	0.871
Biofilm $\pm$ Cu	Supervised	OPLS-DA	1 + 3 + 0	0.944	0.975
Planktonic $\pm$ Cu	Supervised	OPLS-DA	1 + 2 + 0	0.952	0.780

observed for each growth mode. The success of our technique in identifying this dichotomy indicates that it can be used to further examine the effects of toxic stressors and their differential effects on any bacterial biofilms and planktonic cultures, perhaps examining cocontaminant toxic synergy, media effects, and anaerobic growth conditions.

Prior studies have repeatedly demonstrated the increased tolerance/resistance of biofilms to toxic concentrations of metals and attributed this phenomenon to a range of different factors.<sup>2</sup> Our results here suggest that altered metabolism is another factor that could play an important role in decreasing biofilm susceptibility to toxic metals. Many genes in biofilms are expressed differentially compared to planktonic cells, such as those for adherence, EPS production, signaling, and the generation of phenotypically different subpopulations.<sup>1</sup> The presence of heterogeneous cell types within a biofilm could thus be expected to result in large differences between the metabolomes of replicate cultures. Such a phenomenon was not observed, indicated by the close clustering of the biofilm replicate samples in the PCA and PLS-DA analysis, suggesting that the sampling procedure homogenized any metabolic heterogeneity within the biofilm population.

Using unsupervised data analysis techniques (hierarchical clustering and PCA), the difference between control and copper exposed biofilms was easy to discern whereas the planktonic samples remained more or less comparable. While this similarity was not present in the supervised PLS and OPLS-DA models, still it indicates that the effects of copper stress in planktonic cultures are different and less dramatic than in biofilms. This is further supported by each of the SUS plots. The VIP plot shows that the important metabolites are widely different between growth modes and that there are few shared metabolites. Also, the Coefficient plot shows how distinct the two responses are as metabolites deemed significant in each model tended to have smaller coefficients (indicating little change) in the opposite growth mode. These differences indicate that biofilm metabolism undergoes orchestrated changes compared to the dissonant way planktonic cultures react to copper toxicity. While that much is clear, the data contain no indication as to whether the observed metabolic changes are the direct result of copper toxicity or the effect of a cellular response to stress. Biofilms have many general protective mechanisms in order to withstand the effects of toxic metals,<sup>2</sup> whereas planktonic cells are much more vulnerable. Thus, it may be that the observed metabolic changes in biofilms are due to the activation and action of one or more of these mechanisms, whereas the changes seen in the planktonic samples are due to the actual effect of copper ions on the cells. Discerning this difference was beyond the scope of the current study, though if a metabolome similar to the planktonic cultures' could be found in high copper concentration exposed biofilms it may confirm this hypothesis.

The metabolites were separately divided by both the hierarchical clustering and the OPLS-DA VIP scores into those that changed in the planktonic cultures, those that changed in the biofilms, and those that changed in both. This resulted in different but somewhat overlapping categorization of the metabolites. Once categorized, the lists of metabolites were submitted to TICL for analysis in order to infer biological meaning. Because of the exclusion of metabolites with VIP scores below 1, a significant ( $p < 0.05$ ) subnetwork could only be generated from the biofilm list obtained from the OPLS-DA models (data not shown). This supports the idea of the biofilm response being concerted as the ability to generate a subnetwork indicates that the changing metabolites are related and connected. Conversely, this also supports the notion that the planktonic response is generally less concerted.

The enriched pathways identified from the TICL analysis of the lists obtained from the hierarchical clustering allow biological meaning to be inferred about each growth mode and the common response to copper stress. The extracellular-polymeric substance (EPS) of biofilms protects cells in *Pseudomonas aureofaciens* biofilms from copper ions adsorbing to the cell wall by blocking phosphoryl groups that would bind the Cu<sup>2+</sup> ions.<sup>28</sup> Also, biofilms of *P. aeruginosa* were found to chelate Cu<sup>2+</sup> ions within the EPS.<sup>29</sup> Thus, we could expect EPS related metabolism to change in response to copper exposure. Galactose metabolism was altered in biofilms, as was sugar and starch metabolism and the phosphotransferase system, all of which are related to polysaccharide use and transport, which could indicate a change in EPS related metabolism. This is quite likely as the EPS is one of the most distinct features of biofilm physiology and has been largely implicated in the biocide resistance of biofilms.<sup>2,30</sup>

As seen in Table 1, most of the pathways identified in both culture types involve the metabolism of various amino acids. Proteomic analysis of *Pseudomonas putida* planktonic cultures exposed to copper revealed a significant oxidative stress response, including changes to the expression of a number of TCA and glyoxylate cycle proteins.<sup>31</sup> It was also found that the expression of Ts, the guanine nucleotide-exchange factor for elongation factor Tu, to be increased and it was suggested that this was due to increased protein synthesis in response to the copper exposure. The observed shared response to copper indicates a large number of changes in amino acid metabolism and synthesis which could be occurring to help with increased protein synthesis. While both valine, leucine, and isoleucine biosynthesis and alanine, aspartate, and glutamate metabolism were found to be important in the combined response, they were independently identified in the planktonic response. This could indicate that the changes to amino acid metabolism are due to different pathways of toxicity as arginine and proline metabolism was only identified in the biofilm response. In the planktonic cultures, the observed

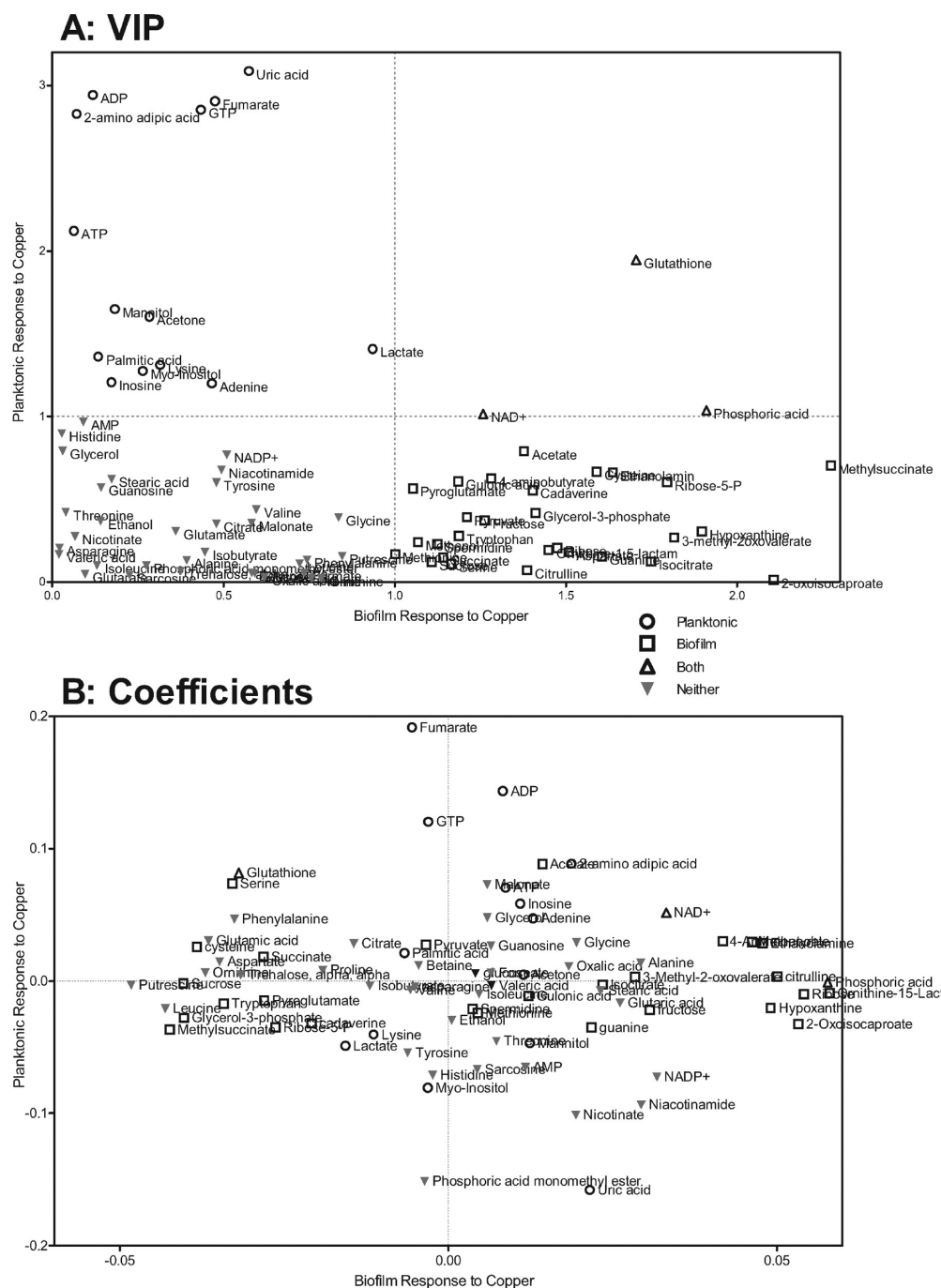


**Figure 3.** Shared-and-unique (SUS) plots of control and copper exposed biofilm and planktonic culture metabolite's variable influence on projection (VIP) scores and coefficients, calculated from separate biofilm and planktonic OPLS-DA models. (A) In the VIP plot, metabolites with a VIP > 1 are deemed important for the response to copper in that culture type. Those in the top right quadrant are important in both responses. (B) In the coefficient plot, metabolite symbols are determined by in which culture their VIP is >1 (open square, biofilm; open circle, planktonic; open triangle, both). Their coefficient value denotes whether they increased (>0) or decreased (<0) in response to copper exposure. Those metabolites with a VIP < 1 were important in neither response (grey triangles).

changes in amino acid metabolism may be due to increased protein synthesis to replace damaged proteins and to synthesize stress proteins, whereas in the biofilm, it may be the result of increased EPS synthesis as proteins are a significant component of EPS.<sup>30</sup>

Glutathione metabolism was also independently identified as important in both the combined and the biofilm response to

copper stress. Changes to glutathione metabolism are to be expected though as it is used as an antioxidant and can also react with metals through its thiol group.<sup>2</sup> The fact that it was identified separately in biofilm metabolism but not planktonic metabolism could indicate that its use as an antioxidant is more prominent in the biofilm lifestyle or that the oxidative stress effects of copper in planktonic cells are beyond the range of



Table 2. Metabolic Pathways Enriched in Response to Copper Exposure Determined by TICL<sup>a</sup>

Planktonic		Both		Biofilm	
metabolic pathway	p-value	metabolic pathway	p-value	metabolic pathway	p-value
Nicotinate and Nicotinamide Metabolism	0.01	Glycine, Serine and Threonine Metabolism	0.01	Arginine and Proline Metabolism	0.01
Pyruvate Metabolism	0.01	Cyanoamino Acid Metabolism	0.01	Phosphotransferase System	0.01
Glycolysis/Gluconeogenesis	0.01	Nitrogen Metabolism	0.01	Lysine Degradation	0.01
Purine Metabolism	0.01	Phenylalanine Metabolism	0.01	Galactose Metabolism	0.01
TCA Cycle	0.01	Glutathione Metabolism	0.01	Glutathione Metabolism	0.01
Alanine, Aspartate and Glutamate Metabolism	0.01	Alanine, Aspartate and Glutamate Metabolism	0.01	Starch and Sucrose Metabolism	0.015
Valine, Leucine and Isoleucine Biosynthesis	0.01	Valine, Leucine and Isoleucine Biosynthesis	0.01		
		Phenylalanine, Tyrosine and Tryptophan Biosynthesis	0.035		

<sup>a</sup>Only pathways with a p-value <0.05 were included, and life-general metabolic pathways (such as aminoacyl-tRNA synthesis) and plant specific pathways were excluded.

protection conferred by increased glutathione synthesis. Monitoring of the actual glutathione levels in each culture type in response to copper could thus be interesting.

The TCA cycle was found by TICL to be altered in response to copper in the planktonic cultures. As previously mentioned, the expression of TCA cycle proteins were modified in *P. putida* and in another study it has been reported that *P. fluorescens* undergoes a rearrangement of the TCA cycle in response to oxidative stress from aluminum, decreasing NADH production in favor of NADPH and oxalate.<sup>31,32</sup> While the TCA cycle changes were observed only in the planktonic cultures, NAD<sup>+</sup> was one of few metabolites that was observed to increase in both culture types in response to copper stress. Related to this, nicotinate and nicotinamide metabolism was affected in the planktonic cultures, though oxalate and NADPH were not observed to increase. This indicates that the oxidative stress induced by copper is not identical, but similar to that of aluminum.

Recently, a number of studies have demonstrated that *P. fluorescens* undergoes a metabolic shift in order to combat oxidative stress.<sup>32,33</sup> The main conclusion of these studies is that several different metabolic networks are carefully manipulated to increase the production of the antioxidant NADPH and decrease the production of the pro-oxidant NADH.<sup>33d</sup> In response to oxidative stress induced mostly by aluminum, but also by hydrogen peroxide, the TCA cycle, glycolysis and gluconeogenesis, in addition to the regulation of several enzymes that consume pyruvate, were found to be altered.<sup>33d</sup> We found the very same networks to be affected in planktonic cultures. Furthermore, nicotinate and nicotinamide metabolism was the top hit in the TICL analysis which indicates that *P. fluorescens* undergoes a similar oxidative stress in response to copper exposure, which is known to be toxic through the generation of reactive oxygen species.<sup>2,16c,27</sup> However, none of these changes were observed in the biofilm response to copper, which was instead characterized by changes in metabolic pathways linked to EPS metabolism. These findings are consistent with a model whereby growth in a biofilm allows the cells to respond in a protective manner; funneling metabolites into EPS synthesis pathways, giving enhanced protection. Planktonic populations do not have this protective mechanism, and therefore, the observed metabolic shifts are a direct consequence of copper toxicity within the cell and the resulting oxidative stress.

In this study, we demonstrate the effectiveness of a novel metabolomics procedure in elucidating global metabolic differences between planktonic and biofilm grown *P. fluorescens* and

their response to copper exposure. These data demonstrate how different the planktonic growth state is to a biofilm and that these states respond quite differently to the antimicrobial stress of a metal ion.

## AUTHOR INFORMATION

### Corresponding Author

\*Dr. Aalim M. Weljie, Department of Biological Sciences, University of Calgary, 2500 University Dr. NW. Calgary, AB Canada, T2N 1N4. E-mail: aweljie@ucalgary.ca. Phone: 403-220-3556.

### Present Addresses

<sup>+</sup>Farncombe Family Digestive Health Research Institute, Department of Medicine, McMaster University, 1280 Main Street West, Hamilton, Ontario, Canada, L8S 4L8.

## ACKNOWLEDGMENT

The Metabolomics Research Centre is supported by the Alberta Cancer Foundation, Alberta Innovates Health Solutions, and the University of Calgary (U of C). M.L.W. was supported by an NSERC Postgraduate Scholarship (Doctoral) and a Ph.D. Studentship from the Alberta Heritage Foundation for Medical Research (AHFMR). S.C.B. was supported by a PURE summer research award from the U of C. H.J.V. is supported as an AHFMR Scientist. This work was funded by Discovery research grants from the Natural Sciences and Engineering Research Council of Canada to H.C., R.J.T., and A.M.W.

## REFERENCES

- (1) López, D.; Vlamakis, H.; Kolter, R. Biofilms. *Cold Spring Harb. Perspect. Biol.* **2010**, 2 (7), No. a000398.
- (2) Harrison, J. J.; Ceri, H.; Turner, R. J. Multimetal resistance and tolerance in microbial biofilms. *Nat. Rev. Microbiol.* **2007**, 5 (12), 928–938.
- (3) Stewart, P. S.; Franklin, M. J. Physiological heterogeneity in biofilms. *Nat. Rev. Microbiol.* **2008**, 6 (3), 199–210.
- (4) Fiehn, O. Metabolomics—The link between genotypes and phenotypes. *Plant Mol. Biol.* **2002**, 48 (1–2), 155–171.
- (5) Vaidyanathan, S. Profiling microbial metabolomes: what do we stand to gain? *Metabolomics* **2005**, 1 (1), 17–28.
- (6) Halouska, S.; Chacon, O.; Fenton, R. J.; Zinniel, D. K.; Barletta, R. G.; Powers, R. Use of NMR metabolomics to analyze the targets of D-cycloserine in mycobacteria: Role of D-alanine racemase. *J. Proteome Res.* **2007**, 6 (12), 4608–4614.

- (7) Sadykov, M. R.; Zhang, B.; Halouska, S.; Nelson, J. L.; Kreimer, L. W.; Zhu, Y.; Powers, R.; Somerville, G. A. Using NMR metabolomics to investigate tricarboxylic acid cycle-dependent signal transduction in *Staphylococcus epidermidis*. *J. Biol. Chem.* **2010**, *285* (47), 36616–36624.
- (8) Gjersing, E. L.; Herberg, J. L.; Horn, J.; Schaldach, C. M.; Maxwell, R. S. NMR metabolomics of planktonic and biofilm modes of growth in *Pseudomonas aeruginosa*. *Anal. Chem.* **2007**, *79* (21), 8037–8045.
- (9) (a) Tremaroli, V.; Workentine, M. L.; Weljie, A. M.; Vogel, H. J.; Ceri, H.; Viti, C.; Tatti, E.; Zhang, P.; Hynes, A. P.; Turner, R. J.; Zannoni, D. Metabolomic investigation of the bacterial response to a metal challenge. *Appl. Environ. Microbiol.* **2009**, *75* (3), 719–28. (b) Workentine, M. L.; Harrison, J. J.; Weljie, A. M.; Tran, V. A.; Stenroos, P. U.; Tremaroli, V.; Vogel, H. J.; Ceri, H.; Turner, R. J. Phenotypic and metabolic profiling of colony morphology variants evolved from *Pseudomonas fluorescens* biofilms. *Environ. Microbiol.* **2010**, *12* (6), 1565–1577.
- (10) Issaq, H. J.; Van, Q. N.; Waybright, T. J.; Muschik, G. M.; Veenstra, T. D. Analytical and statistical approaches to metabolomics research. *J. Sep. Sci.* **2009**, *32* (13), 2183–2199.
- (11) (a) O'Sullivan, D. J.; O'Gara, F. Traits of fluorescent *Pseudomonas* spp. involved in suppression of plant root pathogens. *Microbiol. Rev.* **1992**, *56* (4), 662–676. (b) Paulsen, I. T.; Press, C. M.; Ravel, J.; Kobayashi, D. Y.; Myers, G. S. A.; Mavrodi, D. V.; DeBoy, R. T.; Seshadri, R.; Ren, Q.; Madupu, R.; Dodson, R. J.; Durkin, A. S.; Brinkac, L. M.; Daugherty, S. C.; Sullivan, S. A.; Rosovitz, M. J.; Gwinn, M. L.; Zhou, L.; Schneider, D. J.; Cartinhour, S. W.; Nelson, W. C.; Weidman, J.; Watkins, K.; Tran, K.; Khouri, H.; Pierson, E. A.; Pierson Iii, L. S.; Thomashow, L. S.; Loper, J. E. Complete genome sequence of the plant commensal *Pseudomonas fluorescens* Pf-5. *Nat. Biotechnol.* **2005**, *23* (7), 873–878.
- (12) Workentine, M. L.; Harrison, J. J.; Stenroos, P. U.; Ceri, H.; Turner, R. J. *Pseudomonas fluorescens*' view of the periodic table. *Environ. Microbiol.* **2008**, *10* (1), 238–50.
- (13) Belzile, N.; Wu, G.; Chen, Y.; Appanna, V. Detoxification of selenite and mercury by reduction and mutual protection in the assimilation of both elements by *Pseudomonas fluorescens*. *Sci. Total Environ.* **2006**, *367* (2–3), 704–14.
- (14) (a) Appanna, V. D.; Hamel, R. D.; Léveseur, R. The metabolism of aluminum citrate and biosynthesis of oxalic acid in *Pseudomonas fluorescens*. *Curr. Microbiol.* **2003**, *47* (1), 32–9. (b) Hamel, R.; Appanna, V. Modulation of TCA cycle enzymes and aluminum stress in *Pseudomonas fluorescens*. *J. Inorg. Biochem.* **2001**, *87* (1–2), 1–8. (c) Singh, R.; Beriault, R.; Middaugh, J.; Hamel, R.; Chenier, D.; Appanna, V.; Kalyuzhnyi, S. Aluminum-tolerant *Pseudomonas fluorescens*: ROS toxicity and enhanced NADPH production. *Extremophiles* **2005**, *9* (5), 367–73.
- (15) Sauer, K.; Camper, A. K.; Ehrlich, G. D.; Costerton, J. W.; Davies, D. G. *Pseudomonas aeruginosa* displays multiple phenotypes during development as a biofilm. *J. Bacteriol.* **2002**, *184* (4), 1140–54.
- (16) (a) Harrison, J. J.; Ceri, H.; Stremick, C.; Turner, R. J. Differences in biofilm and planktonic cell mediated reduction of metalloid oxyanions. *FEMS Microbiol. Lett.* **2004**, *235* (2), 357–62. (b) Harrison, J. J.; Ceri, H.; Stremick, C. A.; Turner, R. J. Biofilm susceptibility to metal toxicity. *Environ. Microbiol.* **2004**, *6* (12), 1220–1227. (c) Harrison, J. J.; Tremaroli, V.; Stan, M. A.; Chan, C. S.; Vacchi-Suzzi, C.; Heyne, B. J.; Parsek, M. R.; Ceri, H.; Turner, R. J. Chromosomal antioxidant genes have metal ion-specific roles as determinants of bacterial metal tolerance. *Environ. Microbiol.* **2009**, *11* (10), 2491–2509. (d) Harrison, J. J.; Turner, R. J.; Ceri, H. High-throughput metal susceptibility testing of microbial biofilms. *BMC Microbiol.* **2005**, *5*, 53.
- (17) Bligh, E. G.; Dyer, W. J. A rapid method of total lipid extraction and purification. *Can. J. Biochem. Physiol.* **1959**, *37* (8), 911–917.
- (18) Weljie, A. M.; Newton, J.; Mercier, P.; Carlson, E.; Slupsky, C. M. Targeted profiling: Quantitative analysis of  $^1\text{H}$  NMR metabolomics data. *Anal. Chem.* **2006**, *78* (13), 4430–4442.
- (19) Gullberg, J.; Jonsson, P.; Nordström, A.; Sjöström, M.; Moritz, T. Design of experiments: An efficient strategy to identify factors influencing extraction and derivatization of *Arabidopsis thaliana* samples in metabolomic studies with gas chromatography/mass spectrometry. *Anal. Biochem.* **2004**, *331* (2), 283–295.
- (20) Broeckling, C. D.; Reddy, I. R.; Duran, A. L.; Zhao, X.; Sumner, L. W. MET-IDEA: Data extraction tool for mass spectrometry-based metabolomics. *Anal. Chem.* **2006**, *78* (13), 4334–4341.
- (21) Saeed, A. I.; Bhagabati, N. K.; Braisted, J. C.; Liang, W.; Sharov, V.; Howe, E. A.; Li, J.; Thiagarajan, M.; White, J. A.; Quackenbush, J., TM4Microarray Software Suite. 2006; Vol. 411, pp 134–193.
- (22) van den Berg, R. A.; Hoefsloot, H. C. J.; Westerhuis, J. A.; Smilde, A. K.; van der Werf, M. J., Centering, scaling, and transformations: Improving the biological information content of metabolomics data. *BMC Genomics* **2006**, *7* (142).
- (23) Hummel, J.; Strehmel, N.; Selbig, J.; Walther, D.; Kopka, J. Decision tree supported substructure prediction of metabolites from GC-MS profiles. *Metabolomics* **2010**, *6* (2), 322–333.
- (24) Eriksson, L.; Johansson, E.; Kettaneh-Wold, N.; Wold, S. *Multi- and Megavariate Data Analysis: Principles and Applications*; Umetrics AB: Umea, Sweden, 2001.
- (25) Wiklund, S.; Johansson, E.; Sjöström, L.; Mellerowicz, E. J.; Edlund, U.; Shockcor, J. P.; Gottfries, J.; Moritz, T.; Trygg, J. Visualization of GC/TOF-MS-based metabolomics data for identification of biochemically interesting compounds using OPLS class models. *Anal. Chem.* **2008**, *80* (1), 115–122.
- (26) Antonov, A. V.; Dietmann, S.; Wong, P.; Mewes, H. W. TICL - a web tool for network-based interpretation of compound lists inferred by high-throughput metabolomics. *FEBS J.* **2009**, *276* (7), 2084–2094.
- (27) Teitzel, G. M.; Geddie, A.; De Long, S. K.; Kirisits, M. J.; Whiteley, M.; Parsek, M. R. Survival and growth in the presence of elevated copper: Transcriptional profiling of copper-stressed *Pseudomonas aeruginosa*. *J. Bacteriol.* **2006**, *188* (20), 7242–7256.
- (28) González, A. G.; Shirokova, L. S.; Pokrovsky, O. S.; Emnova, E. E.; Martínez, R. E.; Santana-Casiano, J. M.; González-Dávila, M.; Pokrovski, G. S. Adsorption of copper on *Pseudomonas aureofaciens*: Protective role of surface exopolysaccharides. *J. Colloid Interface Sci.* **2010**, *350* (1), 305–314.
- (29) Harrison, J. J.; Turner, R. J.; Ceri, H. Persister cells, the biofilm matrix and tolerance to metal cations in biofilm and planktonic *Pseudomonas aeruginosa*. *Environ. Microbiol.* **2005**, *7* (7), 981–94.
- (30) Flemming, H. C.; Neu, T. R.; Wozniak, D. J. The EPS matrix: The "house of biofilm cells". *J. Bacteriol.* **2007**, *189* (22), 7945–7947.
- (31) Miller, C. D.; Pettee, B.; Zhang, C.; Pabst, M.; McLean, J. E.; Anderson, A. J. Copper and cadmium: responses in *Pseudomonas putida* KT2440. *Let. Appl. Microbiol.* **2009**, *49* (6), 775–783.
- (32) (a) Chenier, D.; Beriault, R.; Mailloux, R.; Baquie, M.; Abramia, G.; Lemire, J.; Appanna, V. Involvement of fumarase C and NADH oxidase in metabolic adaptation of *Pseudomonas fluorescens* cells evoked by aluminum and gallium toxicity. *Appl. Environ. Microbiol.* **2008**, *74* (13), 3977–3984. (b) Lorenz, M. C.; Singh, R.; Lemire, J.; Mailloux, R. J.; Chénier, D.; Hamel, R.; Appanna, V. D. An ATP and oxalate generating variant tricarboxylic acid cycle counters aluminum toxicity in *Pseudomonas fluorescens*. *PLoS One* **2009**, *4* (10), e7344.
- (33) (a) Beriault, R.; Hamel, R.; Chenier, D.; Mailloux, R.; Joly, H.; Appanna, V. The overexpression of NADPH-producing enzymes counters the oxidative stress evoked by gallium, an iron mimetic. *BioMetals* **2006**, *20* (2), 165–176. (b) Lemire, J.; Kumar, P.; Mailloux, R.; Cossar, K.; Appanna, V. D. Metabolic adaptation and oxaloacetate homeostasis in *P. fluorescens* exposed to aluminum toxicity. *J. Basic Microbiol.* **2008**, *48* (4), 252–259. (c) Lemire, J.; Mailloux, R.; Auger, C.; Whalen, D.; Appanna, V. D. *Pseudomonas fluorescens* orchestrates a fine metabolic-balancing act to counter aluminium toxicity. *Environ. Microbiol.* **2010**, *12* (6), 1384–1390. (d) Mailloux, R. J.; Lemire, J.; Appanna, V. D. Metabolic networks to combat oxidative stress in *Pseudomonas fluorescens*. *Antonie van Leeuwenhoek* **2011**, *99* (3), 433–442. (e) Mailloux, R. J.; Lemire, J.; Kalyuzhnyi, S.; Appanna, V. A novel metabolic network leads to enhanced citrate biogenesis in *Pseudomonas fluorescens* exposed to aluminum toxicity. *Extremophiles* **2008**, *12* (3), 451–459. (f) Mailloux, R. J.; Singh, R.; Brewer, G.; Auger, C.; Lemire, J.; Appanna, V. D. Alpha-ketoglutarate dehydrogenase and glutamate dehydrogenase work in

tandem to modulate the antioxidant alpha-ketoglutarate during oxidative stress in *Pseudomonas fluorescens*. *J. Bacteriol.* **2009**, *191* (12), 3804–3810. (g) Singh, R.; Lemire, J.; Mailloux, R. J.; Appanna, V. D. A novel strategy involved in [corrected] anti-oxidative defense: the conversion of NADH into NADPH by a metabolic network. *PLoS One* **2008**, *3* (7), e2682. (h) Singh, R.; Lemire, J.; Mailloux, R. J.; Chénier, D.; Hamel, R.; Appanna, V. D. An ATP and oxalate generating variant tricarboxylic acid cycle counters aluminum toxicity in *Pseudomonas fluorescens*. *PLoS One* **2009**, *4* (10), e7344.